

Distinguishing genetic correlation from causation across 52 diseases and complex traits

Luke J. O'Connor^{1,2*} and Alkes L. Price^{1,3,4*}

Mendelian randomization, a method to infer causal relationships, is confounded by genetic correlations reflecting shared etiology. We developed a model in which a latent causal variable mediates the genetic correlation; trait 1 is partially genetically causal for trait 2 if it is strongly genetically correlated with the latent causal variable, quantified using the genetic causality proportion. We fit this model using mixed fourth moments $E(\alpha_1^2\alpha_1\alpha_2)$ and $E(\alpha_2^2\alpha_1\alpha_2)$ of marginal effect sizes for each trait; if trait 1 is causal for trait 2, then SNPs affecting trait 1 (large α_1^2) will have correlated effects on trait 2 (large $\alpha_1\alpha_2$), but not vice versa. In simulations, our method avoided false positives due to genetic correlations, unlike Mendelian randomization. Across 52 traits (average $n = 331,000$), we identified 30 causal relationships with high genetic causality proportion estimates. Novel findings included a causal effect of low-density lipoprotein on bone mineral density, consistent with clinical trials of statins in osteoporosis.

Mendelian randomization (MR) is widely used to identify potential causal relationships among heritable traits, potentially leading to new disease interventions^{1–12}. Genetic variants that are significantly associated with one trait, the ‘exposure’, are used as genetic instruments to test for a causal effect on a second trait, the ‘outcome’. If the exposure is causal, then variants affecting the exposure should affect the outcome proportionally. For example, low-density lipoprotein (LDL)^{3,13} and triglycerides⁴ (but not high-density lipoprotein (HDL)³) causally affect coronary artery disease risk. However, pleiotropy presents a challenge for MR, especially when it produces a genetic correlation and when the exposure is highly polygenic^{2,11,12,14–16}. Sometimes, this challenge can be addressed using curated genetic variants without pleiotropic effects; this approach is most appropriate for molecular traits (such as LDL). For other complex traits, statistical approaches have been used to reduce the likelihood of confounding, such as MR-Egger⁷ and bidirectional MR^{11,17,18}. However, these approaches have their own limitations.

We introduce a latent causal variable (LCV) model, under which the genetic correlation between two traits is mediated by a latent variable having a causal effect on each trait. We define trait 1 as partially genetically causal for trait 2 when it is strongly correlated with the causal variable, implying that part of the genetic component of trait 1 is causal for trait 2. We quantify partial causality using the genetic causality proportion. We show in simulations that LCV has major advantages over MR methods, and we apply it to 52 diseases and complex traits.

Results

Overview of methods. The LCV model is based on a latent variable L that mediates the genetic correlation between the two traits (Fig. 1a). Under the LCV model, trait 1 is fully genetically causal for trait 2 if it is perfectly genetically correlated with L ; ‘fully’ means that the entire genetic component of trait 1 is causal for trait 2 (Fig. 1b). More generally, trait 1 is partially genetically causal for trait 2 if the latent variable has a stronger genetic correlation with trait 1 than

with trait 2; ‘partially’ means that part of the genetic component of trait 1 is causal for trait 2. To quantify partial causality, we define the genetic causality proportion (GCP) of trait 1 on trait 2. The GCP ranges between 0 (no partial genetic causality) and 1 (full genetic causality). A high value of GCP (even if it is not exactly 1) implies that interventions targeting trait 1 are likely to affect trait 2. An intermediate value implies that some interventions targeting trait 1 may affect trait 2. (However, we caution that an intervention may fail to mimic genetic perturbations, for example due to its timing relative to disease progression.) For example, a recent study suggested either a fully causal effect of age at menarche (AAM) on height or a shared hormonal pathway affecting both traits¹¹. If this shared pathway (modeled by the LCV, L) has a large effect on AAM but a small effect on height, then AAM would be strictly partially genetically causal for height. Indeed, LCV produced an intermediate GCP estimate ($\bar{GCP} = 0.43$ (s.e. = 0.10); see below). We caution that low GCP estimates are not evidence of full genetic causality, and we refer to trait pairs with low GCP estimates as having limited partial genetic causality. LCV P values test the null hypothesis that $GCP = 0$, and a highly significant P value does not imply a high GCP.

To test for partial genetic causality and to estimate the GCP, we exploit the fact that, if trait 1 is partially genetically causal for trait 2, then most SNPs affecting trait 1 will have proportional effects on trait 2, but not vice versa (Fig. 1c–e). Instead of using thresholds to select subsets of SNPs¹¹, we compare the mixed fourth moments $E(\alpha_1^2\alpha_1\alpha_2)$ and $E(\alpha_2^2\alpha_1\alpha_2)$ of marginal effect sizes (α_1 and α_2 , respectively) for each trait. The rationale for utilizing these mixed fourth moments is that, if trait 1 is causal for trait 2, then SNPs with large effects on trait 1 (large α_1^2) will have proportional effects on trait 2 (large $\alpha_1\alpha_2$), so that $E(\alpha_1^2\alpha_1\alpha_2)$ will be large; conversely, SNPs with large effects on trait 2 (large α_2^2) will generally not affect trait 1 (small $\alpha_1\alpha_2$), so that $E(\alpha_2^2\alpha_1\alpha_2)$ will be smaller. Thus, estimates of the mixed fourth moments can be used to test for partial genetic causality and to estimate the GCP. We note that LCV, unlike MR, does not distinguish between the ‘exposure’ and the ‘outcome’; trait 1 and trait 2 are interchangeable labels.

¹Department of Epidemiology, Harvard T.H. Chan School of Public Health, Boston, MA, USA. ²Program in Bioinformatics and Integrative Genomics, Harvard Graduate School of Arts and Sciences, Cambridge, MA, USA. ³Department of Biostatistics, Harvard T.H. Chan School of Public Health, Boston, MA, USA.

*Program in Medical and Population Genetics, Broad Institute, Cambridge, MA, USA. *e-mail: loconnor@g.harvard.edu; aprince@hsph.harvard.edu

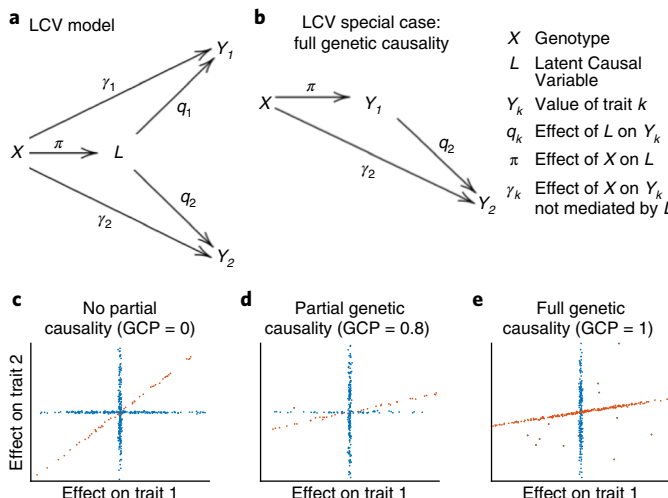


Fig. 1 | Illustration of the LCV model. We display the relationship between genotypes X , LCV L , and trait values Y_1 and Y_2 . **a**, Full LCV model. The genetic correlation between traits Y_1 and Y_2 is mediated by L , which has normalized effects q_1 and q_2 on each trait (see Supplementary Table 17 for a list of random variables versus parameters). **b**, When $q_1=1$, Y_1 is perfectly genetically correlated with L (so L does not need to be shown in the diagram), and we say that Y_1 is fully genetically causal for Y_2 . **c**, Example genetic architecture of genetically correlated traits with no genetic causality ($GCP=0$, that is, $q_2=q_1<1$). Slight noise is added to SNP effects for illustration. Orange SNPs have correlated effects on both traits via L , while blue SNPs do not. **d**, Example genetic architecture of genetically correlated traits with partial genetic causality ($GCP=0.8$, that is, $q_2<q_1<1$). **e**, Example genetic architecture of genetically correlated traits with full genetic causality ($GCP=1$, that is, $q_2<q_1=1$).

LCV assumes that joint effect-size distribution for two traits is a sum of two independent distributions: (1) a shared genetic component corresponding to L , whose values are proportional for both traits, and (2) a distribution that does not contribute to the genetic correlation (see Online Methods). We interpret the first distribution as ‘mediated’ effects (corresponding to π ; Fig. 1a) and the second distribution as ‘direct’ effects (corresponding to γ). The LCV model assumption is strictly weaker than the ‘exclusion restriction’ assumption of MR (see Online Methods).

Under the LCV model, the genetic causality proportion is defined as the number x such that:

$$\frac{q_2^2}{q_1^2} = (\rho_g^2)^x \quad (1)$$

where q_k is the normalized effect of L on trait k (Fig. 1a), and ρ_g is the genetic correlation¹⁶ (note that $\rho_g=q_1q_2$). When the GCP is equal to 1, trait 1 is fully genetically causal for trait 2; when it is positive but less than 1, trait 1 is partially genetically causal. When it is negative, trait 2 is partially genetically causal. The GCP can be defined without making LCV (or other) model assumptions (see Online Methods).

To estimate the GCP, we utilize the following relationship between the mixed fourth moments of the marginal effect-size distribution and the parameters q_1 and q_2 :

$$E(\alpha_1^3\alpha_2) = \kappa_\pi q_1^3 q_2 + 3\rho_g \quad (2)$$

where π is the effect of a SNP on L and $\kappa_\pi = E(\pi^4) - 3$ is the excess kurtosis of π (see Online Methods). This equation implies that, if $|E(\alpha_1^3\alpha_2)| \geq |E(\alpha_1\alpha_2^3)|$, then $q_1^2 \geq q_2^2$ and $GCP \geq 0$.

We calculate statistics $S(x)$ for each possible value of $GCP=x$, using equation (2). These statistics also depend on the heritability¹⁹, the genetic correlation¹⁶, and the cross-trait linkage disequilibrium (LD) score intercept¹⁹. We estimate the variance of these statistics using a block jackknife and obtain an approximate likelihood function for the GCP. We compute a posterior mean GCP estimate (and a posterior standard deviation) using a uniform prior. We test the null hypothesis (that $GCP=0$) using $S(0)$. Details of the method are provided in the Online Methods. We have released open source software implementing the LCV method (see URLs).

Simulations. To compare the calibration and power of LCV with existing causal inference methods, we performed a wide range of null and causal simulations involving simulated summary statistics with no LD. We compared four main methods: LCV, random-effect two-sample MR^{5,9} (denoted MR), MR-Egger⁷, and bidirectional MR¹¹ (see Online Methods). We also compared LCV with the weighted median estimator (MR-WME)⁸ and mode-based estimator (MR-MBE)¹⁰ (whose performances were roughly similar to MR and MR-Egger, respectively; results using these methods are reported in the supplementary tables). We applied each method to simulated genome-wide association study (GWAS) summary statistics ($n=100,000$ individuals in each of two non-overlapping cohorts; $M=50,000$ independent SNPs²⁰) for two heritable traits ($h^2=0.3$), generated under the LCV model. LCV uses LD score regression¹⁹; for simulations with no LD, we use constrained-intercept LD score regression (simulations with LD are described below). A detailed description of all simulations is provided in the Supplementary Note, and simulation parameters are described in Supplementary Table 1.

First, we performed null simulations ($GCP=0$) with uncorrelated pleiotropic effects (via γ ; Fig. 1a) and zero genetic correlation. Of the SNPs, 1% were causal for both traits (with independent effect sizes, explaining 20% of heritability for each trait), and 4% were causal for each trait exclusively (Fig. 2a and Supplementary Table 2a–d). LCV produced conservative P values (0.0% false positive rate at $\alpha=0.05$); our normalization of the test statistic can lead to conservative P values when the genetic correlation is low (see Online Methods). All three main MR methods produced well-calibrated P values. Even though the ‘exclusion restriction’ assumption of MR is violated here, these results confirm that uncorrelated pleiotropic effects do not confound random-effect MR at large sample size²¹. (Such pleiotropy is known to cause false positives if a less conservative fixed-effect approach is used²².) In these simulations, all methods except LCV used the set of approximately 170 SNPs (on average) that were genome-wide significant ($P < 5 \times 10^{-8}$) for trait 1 (or approximately 330 SNPs that were genome-wide significant for either trait, in the case of bidirectional MR).

Second, we performed null simulations with a non-zero genetic correlation. Of the SNPs, 1% had causal effects on L , and L had effects $q_1=q_2=\sqrt{0.2}$ on each trait (so that $\rho_g=0.2$); 4% were causal for each trait exclusively (Fig. 2b and Supplementary Table 2e–g). MR and MR-Egger both produced excess false positives, while bidirectional MR and LCV produced well-calibrated P values. These simulations violate the MR-Egger assumption that the magnitude of pleiotropic effects on trait 2 are independent of the magnitude of effects on trait 1 (the ‘InSIDE’ assumption)⁷, as SNPs with larger effects on L have larger effects on both trait 1 and trait 2 on average, consistent with known limitations²².

Third, we performed null simulations with a non-zero genetic correlation and differential polygenicity in the non-shared genetic architecture between the two traits. Of the SNPs, 1% were causal for L , with effects $q_1=q_2=\sqrt{0.2}$ on each trait; 2% were causal for trait 1 but not trait 2; and 8% were causal for trait 2 but not trait 1 (Fig. 2c and Supplementary Table 2h–j). Thus, the likelihood that a SNP would be genome-wide significant was higher for causal SNPs

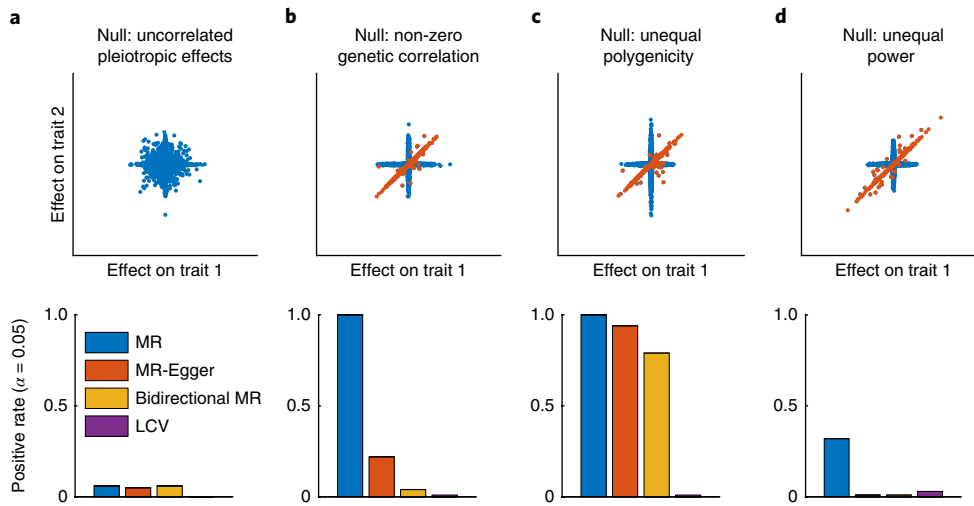


Fig. 2 | Null simulations with no LD to assess calibration. We compared LCV with three main MR methods (two-sample MR, MR-Egger, and bidirectional MR). We report the positive rate ($\alpha = 0.05$) for a causal (or partially causal) effect. Scatterplots illustrate the bivariate effect-size distribution. **a**, Null simulation ($GCP = 0$) with uncorrelated pleiotropic effects and zero genetic correlation. **b**, Null simulation with non-zero genetic correlation. **c**, Null simulation with non-zero genetic correlation and differential polygenicity between the two traits. **d**, Null simulation with non-zero genetic correlation and differential power for the two traits. Results for each panel are based on 4,000 simulations. Numerical results are reported in Supplementary Table 1.

affecting trait 1 only than for causal SNPs affecting trait 2 only. As a result of this imbalance, bidirectional MR (as well as other MR methods) produced excess false positives, unlike LCV.

Fourth, we performed null simulations with a non-zero genetic correlation and differential power for the two traits, reducing the sample size from 100,000 to 20,000 for trait 2. Of the SNPs, 0.5% were causal for L , with effects $q_1 = q_2 = \sqrt{0.5}$ on each trait, and 8% were causal for each trait exclusively (Fig. 2d and Supplementary Table 2k–m). Because per-SNP heritability was higher for shared causal SNPs than for non-shared causal SNPs, shared causal SNPs were more likely to reach genome-wide significance in the smaller trait 1 sample ($n=20,000$), leading to a similar imbalance as in Fig. 2c. As a result, bidirectional MR (as well as other MR methods) produced excess false positives, while LCV produced well-calibrated P values.

Next, we performed causal simulations (with full genetic causality) to assess whether LCV is well powered to detect a causal effect. We caution that LCV had lower power in simulations with LD (see below). First, we chose a set of default parameters: $n=25,000$ for each trait, 5% of SNPs causal for trait 1 (the causal trait), a (fully) causal effect of size $q_2=0.2$ of trait 1 on trait 2, and 5% of SNPs causal for trait 2 only (Fig. 3a). There were ~15 genome-wide significant SNPs on average, explaining ~2% of h^2 . LCV was well powered to detect a causal effect at $\alpha=0.001$, while MR had lower power and bidirectional MR and MR-Egger had very low power.

Second, we reduced the sample size for trait 1 (Fig. 3b and Supplementary Table 3b–d), finding that LCV had high power while the MR methods had very low power, owing to the small number of genome-wide significant SNPs. We caution that, for real traits, heritability estimates can be noisy at very low sample size, potentially leading to unreliable results (see Supplementary Note and “Application to real traits”, below).

Third, we reduced the sample size for trait 2 (Fig. 3c and Supplementary Table 3e–g). LCV had high power, while other methods had low power. The effect of trait 2 sample size on MR power was more modest than the effect of trait 1 sample size, suggesting that the number of genome-wide significant SNPs (ascertained using trait 1) is the primary limiting factor for MR power.

Fourth, we reduced the causal effect size of trait 1 on trait 2 (Fig. 3d and Supplementary Table 3h–j). LCV had low power, and

other methods had very low power. Fifth, we increased the polygenicity of the causal trait (Fig. 3e and Supplementary Table 3k–m). LCV had moderate power, while the MR methods had very low power, again owing to the low number of genome-wide significant SNPs. We also simulated a partially genetically causal relationship ($GCP=0.25–0.75$), with similar results (Supplementary Table 3p–r). We compared our GCP estimates in fully causal simulations with our GCP estimates in partially causal simulations, finding that LCV reliably distinguished the two cases, unlike existing methods (Supplementary Table 3a,p–r).

To investigate potential limitations of our approach, we performed null and causal simulations under genetic architectures that violate LCV model assumptions. These simulations and their results are described in detail in the Supplementary Note. We simulated four types of LCV model violations: (1) null simulations with a bivariate Gaussian mixture model, where one of the mixture components generates imperfectly correlated effect sizes on the two traits; (2) null simulations with two LCVs; (3) causal simulations with a bivariate Gaussian mixture model; and (4) causal simulations with an additional latent confounder. LCV produced well-calibrated P values under models of type 1 (Supplementary Fig. 1a–c); in addition, these simulations recapitulated the limitations of existing methods (Fig. 2). Models of type 2 sometimes caused LCV (and existing methods) to produce false positives (Supplementary Fig. 1d,e); however, extreme values of the simulation parameters were required for LCV to produce high GCP estimates, implying that results with high GCP estimates are extremely unlikely to be false positives (Supplementary Fig. 2). Causal models of type 3 and type 4 lead to reduced power for LCV (and other methods; Supplementary Fig. 1f,g), as well as downwardly biased GCP estimates for LCV (Supplementary Tables 4 and 5).

Next, we performed simulations with real LD patterns to further assess the robustness of the LCV method. These simulations and their results are described in detail in the Supplementary Note. In null simulations with a wide range of parameter settings, LCV produced approximately well-calibrated or conservative false positive rates, except for simulations at low sample size with noisy heritability estimates (Supplementary Tables 6a–s and 7). (We exclude real datasets with noisy heritability estimates.) We determined that LCV can be confounded by uncorrected population

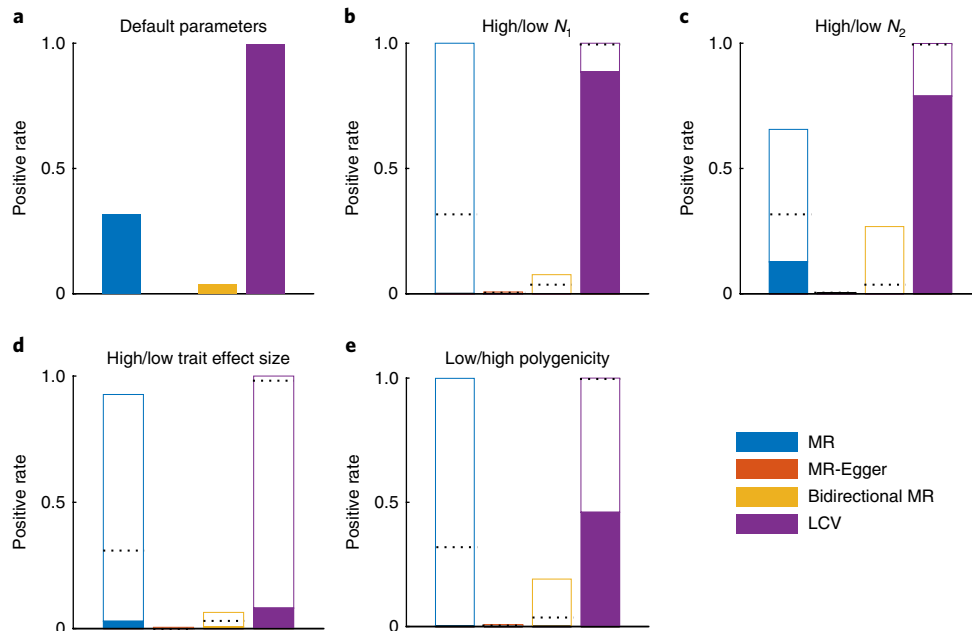


Fig. 3 | Causal simulations with no LD to assess power. We compared LCV with three main MR methods (two-sample MR, MR-Egger and bidirectional MR). We report the positive rate ($\alpha = 0.001$) for a causal (or partially causal) effect. **a**, Causal simulations with default parameters: $N_1 = N_2 = 25,000$; $M = 50,000$; $q_1 = 1$, $q_2 = 0.2$ (results also displayed as dashed lines in **b–e**). **b**, Higher (unfilled) or lower (filled) sample size for trait 1 ($N_1 = 50,000$ and $N_1 = 12,500$, respectively). **c**, Higher (unfilled) or lower (filled) sample size for trait 2 ($N_2 = 50,000$ and $N_2 = 12,500$, respectively). **d**, Higher (unfilled) or lower (filled) causal effect size of trait 1 on trait 2 ($q_2 = 0.4$ and $q_2 = 0.1$, respectively). **e**, Lower (unfilled) or higher (filled) polygenicity for trait 1. Results for each panel are based on 1,000 simulations. Numerical results are reported in Supplementary Table 3.

stratification (Supplementary Table 8). In non-null simulations, LCV was usually well powered to detect a causal or partially causal effect (Supplementary Table 6t–bb). In simulations with a range of GCP values, we determined that our posterior mean GCP estimates are approximately unbiased and that our posterior standard errors are approximately well calibrated (Supplementary Fig. 3 and Supplementary Table 9).

Application to real traits. We applied LCV and the MR methods to GWAS summary statistics for 52 diseases and complex traits, including summary statistics for 37 UK Biobank traits^{23,24} computed using BOLT-LMM²⁵ (average $n = 429,000$) and 15 other traits (average $n = 54,000$) (see Supplementary Table 10 and Online Methods). These traits were selected on the basis of the significance of their heritability estimates ($Z_h > 7$), and trait pairs with very high genetic correlations ($|r_{g,ij}| > 0.9$) were pruned. As in previous work, we excluded the major histocompatibility complex region from all analyses, due to its unusually large effect sizes and long-range LD patterns¹⁹.

We applied LCV to the 429 trait pairs (32% of all trait pairs) with a nominally significant genetic correlation ($P < 0.05$), detecting significant evidence of full or partial genetic causality for 59 trait pairs ($FDR < 1\%$), including 30 trait pairs with $GCP > 0.6$. We primarily focus on trait pairs with high GCP estimates, which have greater biological interest (and are extremely unlikely to be false positives; see “Simulations”). Results for selected trait pairs are displayed in Fig. 4, results for the 30 trait pairs with $GCP > 0.6$ are reported in Table 1, results for all 59 significant trait pairs are reported in Supplementary Table 11, and results for all 429 genetically correlated trait pairs are reported in Supplementary Table 12. To investigate the possibility that these results could be affected by model misspecification, we developed an auxiliary test for partial genetic causality that does not rely on LCV model assumptions (Supplementary Note). This test, though underpowered, produces highly concordant results on these

trait pairs, confirming that LCV is unlikely to be affected by model misspecification.

Myocardial infarction (MI) had a nominally significant genetic correlation with 31 other traits, of which six had significant evidence ($FDR < 1\%$) for a fully or partially genetically causal effect on MI (Table 1); there was no evidence for a genetically causal effect of MI on any other trait. Consistent with previous studies, these traits included LDL^{3,13}, triglycerides⁴, and body mass index (BMI)²⁶, but not HDL³. The effect of BMI was also consistent with previous MR studies^{26–29}, although these studies did not attempt to account for pleiotropic effects (also see ref. ³⁰, which detected no effect). There was also evidence for a genetically causal effect of high cholesterol, which was unsurprising (due to the high genetic correlation with LDL) but noteworthy because of its strong genetic correlation with MI, compared with LDL and triglycerides. The result for HDL and MI did not pass our significance threshold ($FDR < 1\%$) but was nominally significant ($P = 0.02$; Supplementary Table 12); we residualized HDL summary statistics on summary statistics for three established causal risk factors (LDL, BMI, and triglycerides), determining that residualized HDL showed no evidence of genetic causality ($P = 0.8$). However, most of the other traits remained significant (Supplementary Table 13).

We also detected evidence for a fully or partially genetically causal effect of hypothyroidism on MI (Table 1). Although hypothyroidism is not as well established a cardiovascular risk factor as high LDL, its genetic correlation with MI is comparable (Table 1), and this effect is mechanistically plausible^{31,32}. While this result was robust in the conditional analysis (Supplementary Table 13), and there was no strong evidence for a genetically causal effect of hypothyroidism on lipid traits (Supplementary Table 12), it is possible that this effect is mediated by lipid traits. A recent MR study of thyroid hormone levels, at $\sim 20\times$ lower sample size than the present study, provided evidence for a genetically causal effect on LDL but not coronary artery disease³³. However, clinical trials have demonstrated that

treatment of subclinical hypothyroidism leads to improvement in several cardiovascular risk factors^{34–38}. We also detected evidence for a fully or partially genetically causal effect of hypothyroidism on type 2 diabetes (Supplementary Table 11), consistent with a longitudinal association between subclinical hypothyroidism and diabetes incidence³⁹, as well as an effect of thyroid hormone withdrawal on glucose disposal in athyreotic patients⁴⁰.

We detected evidence for a (negative) genetically causal effect of LDL on bone mineral density (BMD; Table 1). A meta-analysis of randomized clinical trials reported that statin administration increases BMD⁴¹. Moreover, familial defective apolipoprotein B leads to high LDL and low BMD⁴². We performed two-sample MR using eight SNPs that were previously curated (in ref. 3; see Supplementary Note), finding modest evidence for a negative causal effect ($P=0.04$). Because these variants are not likely to have pleiotropic effects, this analysis provides separate evidence for a genetically causal effect. Additional trait pairs with high GCP estimates are discussed in the Supplementary Note.

Approximately half of significant trait pairs had low to medium GCP estimates (<0.6). Given that there is lower power to detect trait pairs with low GCP values (Supplementary Table 3a,p–r), it is likely that partial genetic causality with $GCP < 0.6$ is more common than full or nearly full genetic causality with $GCP > 0.6$. Trait pairs with low GCP estimates can suggest plausible biological hypotheses. For example, we identified a partially genetically causal effect of AAM on height ($\widehat{GCP} = 0.43(0.10)$; Supplementary Table 11), suggesting that these traits are influenced by a shared hormonal pathway that is more strongly correlated with AAM than with height, as recently hypothesized¹¹.

A recent study reported genetic correlations between various complex traits and number of children in males and females⁴³. We identified only one trait (balding in males) with a fully or partially causal effect on number of children (in males; Table 1). For college education, which has a strong negative genetic correlation with number of children ($\widehat{\rho}_g = -0.31(0.07)$ and $-0.26(0.06)$ in males and females, respectively), we obtained low GCP estimates with low standard errors ($\widehat{GCP} = 0.00(0.09)$ and $\widehat{GCP} = 0.04(0.21)$, respectively; Supplementary Table 12). Thus, a genetic correlation with number of children does not imply direct selection. This result does not contradict the conclusion⁴³ that complex traits are affected by natural selection, as pleiotropic selection can also affect a trait⁴⁴.

Polygenic autism risk is positively genetically correlated with educational attainment¹⁶ (and cognitive ability⁴⁵, a highly genetically correlated trait⁴⁶), possibly consistent with the hypothesis that common autism risk variants persist in the population due to compensatory effects on cognitive ability^{47,48}. If so, then most common variants affecting autism risk would also affect educational attainment, leading to a partially genetically causal effect of autism on educational attainment. However, we detected evidence against such an effect ($\widehat{GCP} = 0.13(0.13)$, $\widehat{\rho}_g = 0.23(0.07)$; Supplementary Table 12). Additional trait pairs with negative results are reported in the Supplementary Note and in Supplementary Table 14.

To evaluate whether the limitations of MR observed in simulations (Fig. 2) are also observed in analyses of real traits, we applied MR, MR-Egger, and bidirectional MR to all 429 genetically correlated trait pairs (Supplementary Table 12). MR reported significant causal relationships (1% FDR) for 271 of 429 trait pairs, including 155 pairs of traits for which each trait was reported to be causal for the other trait. This implausible result confirms that MR frequently produces false positives in the presence of a genetic correlation, as predicted by our simulations (Fig. 2). In contrast, LCV reported a significant partially or fully genetically causal relationship for only 59 trait pairs (Supplementary Table 11), and it never reports a causal effect in both directions. Similarly, bidirectional MR reported a significant causal relationship for only 45

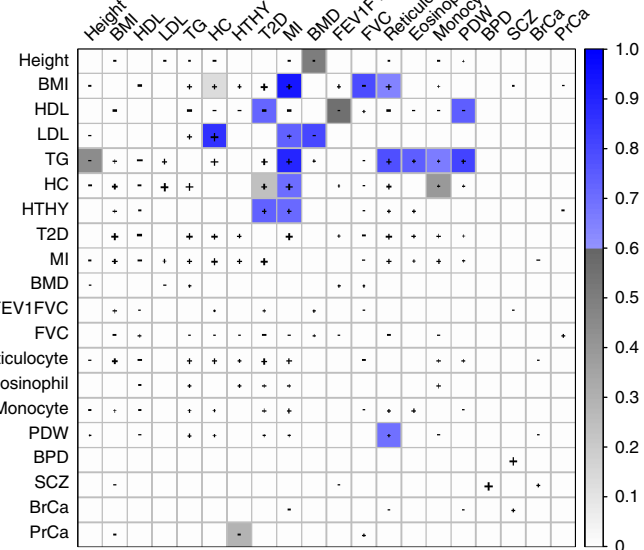


Fig. 4 | Partially or fully genetically causal relationships between selected complex traits. Shaded squares indicate significant evidence for a causal or partially causal effect of the row trait on the column trait (FDR < 1%). Color scale indicates posterior mean \widehat{GCP} for the effect of the row trait on the column trait; blue color indicates $\widehat{GCP} > 0.6$, gray color indicates $\widehat{GCP} < 0.6$. Plus or minus signs indicate trait pairs with a nominally significant positive or negative genetic correlation ($P < 0.05$); the size of the symbol is proportional to strength of the genetic correlation. Results for the 30 trait pairs with $\widehat{GCP} > 0.6$ are reported in Table 1, results for all 59 significant trait pairs are reported in Supplementary Table 11, and results for all 429 genetically correlated trait pairs are reported in Supplementary Table 12. TG, triglycerides; HC, high cholesterol; HTHY, hypothyroidism; T2D, type II diabetes; FEV1FVC, ratio of forced expiratory volume to forced vital capacity; PDW, platelet distribution width; BPD, bipolar disorder; SCZ, schizophrenia; BrCa, breast cancer; PrCa, prostate cancer.

trait pairs (including 17 pairs of traits that overlapped with LCV; Supplementary Table 15).

Discussion

We have introduced an LCV model to identify causal relationships among genetically correlated pairs of complex traits. We applied LCV to 52 traits, finding that many trait pairs do exhibit partially or fully genetically causal relationships. Our method represents an advance for two main reasons. First, unlike existing MR methods, LCV reliably distinguishes between genetic correlation and full or partial genetic causation. Positive findings using LCV are more likely to reflect true causal effects. Second, we define and estimate the GCP to quantify the degree of causality. This parameter, which provides information orthogonal to the genetic correlation or the causal effect size, enables a non-dichotomous description of the causal architecture.

This study has two important limitations (additional limitations are discussed in the Supplementary Note). First, the LCV model includes only a single intermediary and can be confounded in the presence of multiple intermediaries⁴⁹. However, the 30 trait pairs with $\widehat{GCP} > 0.6$ are unlikely to be false positives (see Supplementary Note and Supplementary Fig. 2). Second, because LCV models only two traits at a time, it cannot be used to identify conditional effects given observed confounders⁵⁰. This approach was used, for example, to show that triglycerides affect coronary artery disease risk conditional on LDL⁴. However, it is less essential for LCV to model observed genetic confounders, since LCV explicitly models a latent genetic confounder⁵¹.

Table 1 | Fully or partially genetically causal relationships between complex traits

Trait 1	Trait 2	P_{LCV}	$\hat{\rho}_g$ (s.e.)	\widehat{GCP} (s.e.)	MR reference
Triglycerides	Hypertension	1×10^{-38}	0.25 (0.04)	0.95 (0.04)	
BMI	Myocardial infarction	5×10^{-9}	0.34 (0.09)	0.94 (0.11)	28,57
Triglycerides	Myocardial infarction	2×10^{-31}	0.30 (0.06)	0.90 (0.08)	4
Triglycerides	Blood pressure (systolic)	1×10^{-40}	0.13 (0.03)	0.89 (0.08)	
HDL	Hypertension	1×10^{-21}	-0.29 (0.06)	0.87 (0.09)	
LDL	High cholesterol	2×10^{-6}	0.77 (0.07)	0.86 (0.11)	
Triglycerides	Mean cell volume	2×10^{-18}	-0.20 (0.04)	0.86 (0.11)	
Triglycerides	Blood pressure diastolic	9×10^{-39}	0.11 (0.04)	0.86 (0.10)	
Mean platelet volume	Platelet count	1×10^{-9}	-0.66 (0.03)	0.84 (0.10)	
BMI	Hypertension	3×10^{-16}	0.38 (0.03)	0.83 (0.11)	11,57
Triglycerides	Platelet distribution width	1×10^{-16}	0.19 (0.04)	0.81 (0.13)	
LDL	BMD (heel)	7×10^{-34}	-0.12 (0.05)	0.80 (0.12)	
BMI	Forced vital capacity	9×10^{-13}	-0.22 (0.03)	0.79 (0.17)	
High cholesterol	Red blood cell count	0.002	0.08 (0.03)	0.79 (0.15)	
Triglycerides	Reticulocyte count	5×10^{-10}	0.33 (0.05)	0.79 (0.14)	
Type 2 diabetes	Mean cell volume	0.004	-0.15 (0.03)	0.77 (0.20)	
HDL	Red blood cell count	0.003	-0.13 (0.05)	0.76 (0.34)	
Triglycerides	Eosinophil count	6×10^{-17}	0.14 (0.05)	0.75 (0.16)	
Balding	Number of children (male)	3×10^{-30}	-0.16 (0.05)	0.75 (0.13)	
HDL	Platelet distribution width	2×10^{-16}	-0.14 (0.04)	0.75 (0.16)	
Red blood cell distribution width	Type 2 diabetes	7×10^{-4}	0.11 (0.03)	0.73 (0.19)	
LDL	Myocardial infarction	4×10^{-31}	0.17 (0.08)	0.73 (0.13)	3,13
High cholesterol	Lymphocyte count	0.004	0.18 (0.04)	0.73 (0.22)	
Platelet distribution width	Platelet count	2×10^{-7}	-0.47 (0.04)	0.73 (0.15)	
Hypothyroidism	Type 2 diabetes	4×10^{-4}	0.22 (0.05)	0.73 (0.29)	
HDL	Type 2 diabetes	5×10^{-7}	-0.40 (0.06)	0.72 (0.17)	
Myocardial infarction	Breast cancer	0.01	-0.16 (0.05)	0.72 (0.24)	
Hypothyroidism	Myocardial infarction	1×10^{-11}	0.26 (0.05)	0.72 (0.16)	
High cholesterol	Myocardial infarction	5×10^{-4}	0.52 (0.12)	0.71 (0.19)	
HDL	Blood pressure (diastolic)	9×10^{-17}	-0.12 (0.06)	0.70 (0.18)	

We report all significant trait pairs (1% FDR) with high GCP estimates ($\widehat{GCP} > 0.6$). P_{LCV} is the P value for the null hypothesis of no partial genetic causality; $\hat{\rho}_g$ is the estimated genetic correlation, with standard error; GCP is the posterior mean estimated genetic causality proportion, with posterior standard error. We provide references for all MR studies supporting causal relationships between these traits that we are currently aware of. Results for all 59 significant trait pairs are reported in Supplementary Table 11, and results for all 429 genetically correlated trait pairs are reported in Supplementary Table 12.

Despite these limitations, for most pairs of complex traits, we recommend using LCV instead of MR, as MR methods (including MR-Egger) are easily confounded by genetic correlations. MR is more reliable when it is possible to identify variants that are likely to represent valid instruments. For example, an MR analysis identified a causal effect of vitamin D on multiple sclerosis, utilizing genetic variants near genes with well-characterized effects on vitamin D synthesis, metabolism, and transport⁵². As another example, cis-eQTLs can be used as genetic instruments, as they are unlikely to be confounded by processes mediated in trans^{53–55}, however, this approach has other limitations^{54,56}.

URLs. Open-source software implementing our method is available at <https://github.com/lukejConnor/LCV>.

Online content

Any methods, additional references, Nature Research reporting summaries, source data, statements of data availability and associated accession codes are available at <https://doi.org/10.1038/s41588-018-0255-0>.

Received: 23 October 2017; Accepted: 13 September 2018;
Published online: 29 October 2018

References

1. Davey Smith, G. & Ebrahim, S. Mendelian randomization: can genetic epidemiology contribute to understanding environmental determinants of disease? *Int. J. Epidemiol.* **32**, 1–22 (2003).
2. Davey Smith, G. & Hemani, G. Mendelian randomization: genetic anchors for causal inference in epidemiological studies. *Hum. Mol. Genet.* **23**, R89–R98 (2014).
3. Voight, B. F. et al. Plasma HDL cholesterol and risk of myocardial infarction: a Mendelian randomisation study. *Lancet* **380**, 572–580 (2012).
4. Do, R. et al. Common variants associated with plasma triglycerides and risk for coronary artery disease. *Nat. Genet.* **45**, 1345–1352 (2013).
5. Burgess, S., Butterworth, A. & Thompson, S. G. Mendelian randomization analysis with multiple genetic variants using summarized data. *Genet. Epidemiol.* **37**, 658–665 (2013).
6. Kang, H. et al. Instrumental variables estimation with some invalid instruments and its application to Mendelian randomization. *J. Am. Stat. Assoc.* **111**, 132–144 (2016).
7. Bowden, J., Davey Smith, G. & Burgess, S. Mendelian randomization with invalid instruments: effect estimation and bias detection through Egger regression. *Int. J. Epidemiol.* **44**, 512–525 (2015).

8. Bowden, J. et al. Consistent estimation in Mendelian randomization with some invalid instruments using a weighted median estimator. *Genet. Epidemiol.* **40**, 304–314 (2016).
9. Hemani, G. et al. The MR-Base platform supports systematic causal inference across the genome. *eLife* **7**, e34408 (2018).
10. Hartwig, F. P., Davey Smith, G. & Bowden, J. Robust inference in summary data Mendelian randomization via the zero modal pleiotropy assumption. *Int. J. Epidemiol.* **46**, 1985–1998 (2017).
11. Pickrell, J. K. et al. Detection and interpretation of shared genetic influences on 42 human traits. *Nat. Genet.* **48**, 709–717 (2016).
12. Verbanck, M., Chen, C. Y., Neale, B. & Do, R. Detection of widespread horizontal pleiotropy in causal relationships inferred from Mendelian randomization between complex traits and diseases. *Nat. Genet.* **50**, 693–698 (2018).
13. Cohen, J. C., Boerwinkle, E., Mosley, T. H. Jr & Hobbs, H. H. Sequence variations in PCSK9, low LDL, and protection against coronary heart disease. *N. Engl. J. Med.* **354**, 1264–1272 (2006).
14. Paaby, A. B. & Rockman, M. V. The many faces of pleiotropy. *Trends Genet.* **29**, 63–73 (2013).
15. VanderWeele, T. J. et al. Methodological challenges in Mendelian randomization. *Epidemiology* **25**, 427–435 (2014).
16. Bulik-Sullivan, B. et al. An atlas of genetic correlations across human diseases and traits. *Nat. Genet.* **47**, 1236–1241 (2015).
17. Welsh, P. et al. Unraveling the directional link between adiposity and inflammation: a bidirectional Mendelian randomization approach. *J. Clin. Endocrinol. Metab.* **95**, 93–99 (2010).
18. Vimalesarwan, K. S. et al. Causal relationship between obesity and vitamin D status: bi-directional Mendelian randomization analysis of multiple cohorts. *PLoS Med.* **10**, e1001383 (2013).
19. Bulik-Sullivan, B. K. et al. LD score regression distinguishes confounding from polygenicity in genome-wide association studies. *Nat. Genet.* **47**, 291–295 (2015).
20. Yang, J. et al. Genetic variance estimation with imputed variants finds negligible missing heritability for human height and body mass index. *Nat. Genet.* **47**, 1114–1120 (2015).
21. Kolesar, M. et al. Identification and inference with many invalid instruments. *J. Bus. Econ. Stat.* **33**, 474–484 (2015).
22. Burgess, S. & Thompson, S. G. Interpreting findings from Mendelian randomization using the MR-Egger method. *Eur. J. Epidemiol.* **32**, 377–389 (2017).
23. Sudlow, C. et al. UK Biobank: an open access resource for identifying the causes of a wide range of complex diseases of middle and old age. *PLoS Med.* **12**, e1001779 (2015).
24. Croft, C. et al. Genome-wide genetic data on ~500,000 UK Biobank participants. Preprint at bioRxiv <https://doi.org/10.1101/166298> (2017).
25. Loh, P. R. et al. Mixed-model association for biobank-scale datasets. *Nat. Genet.* **50**, 906–908 (2018).
26. Holmes, M. V., Ala-Korpela, M. & Davey Smith, G. Mendelian randomization in cardiometabolic disease: challenges in evaluating causality. *Nat. Rev. Cardiol.* **14**, 577–590 (2017).
27. Davey Smith, G. et al. The association between BMI and mortality using offspring BMI as an indicator of own BMI: large intergenerational mortality study. *BMJ* **339**, b5043 (2009).
28. Nordestgaard, B. G. et al. The effect of elevated body mass index on ischemic heart disease risk: causal estimates from a Mendelian randomisation approach. *PLoS Med.* **9**, e1001212 (2012).
29. Hägg, S. et al. Adiposity as a cause of cardiovascular disease: a Mendelian randomization study. *Int. J. Epidemiol.* **44**, 578–586 (2015).
30. Holmes, M. V. et al. Causal effects of body mass index on cardiometabolic traits and events: a Mendelian randomization analysis. *Am. J. Hum. Genet.* **94**, 198–208 (2014).
31. Klein, I. & Ojamaa, K. Thyroid hormone and the cardiovascular system. *N. Engl. J. Med.* **344**, 501–509 (2001).
32. Grais, I. M. & Sowers, J. R. Thyroid and the heart. *Am. J. Med.* **127**, 691–698 (2014).
33. Zhao, J. V. & Schooling, C. M. Thyroid function and ischemic heart disease: a Mendelian randomization study. *Sci. Rep.* **7**, 8515 (2017).
34. Monzani, F. et al. Effect of levothyroxine on cardiac function and structure in subclinical hypothyroidism: double blind, placebo-controlled study. *J. Clin. Endocrinol. Metab.* **86**, 1110–1115 (2001).
35. Meier, C. et al. TSH-controlled L-thyroxine therapy reduces cholesterol levels and clinical symptoms in subclinical hypothyroidism: a double blind, placebo-controlled trial (Basel Thyroid Study). *J. Clin. Endocrinol. Metab.* **86**, 4430–4863 (2001).
36. Monzani, F. et al. Effect of levothyroxine replacement on lipid profile and intima-media thickness in subclinical hypothyroidism: a double-blind, placebo-controlled study. *J. Clin. Endocrinol. Metab.* **89**, 2099–2106 (2004).
37. Razvi, S. et al. The beneficial effect of L-thyroxine on cardiovascular risk factors, endothelial function, and quality of life in subclinical hypothyroidism: randomized, crossover trial. *J. Clin. Endocrinol. Metab.* **92**, 1715–1723 (2007).
38. Nagasaki, T. et al. Decrease of brachial-ankle pulse wave velocity in female subclinical hypothyroid patients during normalization of thyroid function: a double-blind, placebo-controlled study. *Eur. J. Endocrinol.* **160**, 409–415 (2009).
39. Chaker, L. et al. Thyroid function and risk of type 2 diabetes: a population-based prospective cohort study. *BMC Med.* **14**, 150 (2016).
40. Brenta, G. et al. Acute thyroid hormone withdrawal in athyreotic patients results in a state of insulin resistance. *Thyroid* **19**, 665–669 (2009).
41. Wang, Z. et al. Effects of statins on bone mineral density and fracture risk: a PRISMA-compliant systematic review and meta-analysis. *Medicine* **95**, e3042 (2016).
42. Yerges, L. M. et al. Decreased bone mineral density in subjects carrying familial defective apolipoprotein B-100. *J. Clin. Endocrinol. Metab.* **98**, E1999–E2005 (2013).
43. Sanjak, J. S. et al. Evidence of directional and stabilizing selection in contemporary humans. *Proc. Natl Acad. Sci. USA* **115**, 151–156 (2018).
44. Price, G. R. Selection and covariance. *Nature* **227**, 520–521 (1970).
45. Clarke, T. K. et al. Common polygenic risk for autism spectrum disorder (ASD) is associated with cognitive ability in the general population. *Mol. Psychiatry* **21**, 419–425 (2016).
46. Davies, G. et al. Genome-wide association study of cognitive functions and educational attainment in UK Biobank ($N=112,151$). *Mol. Psychiatry* **21**, 758–767 (2016).
47. Keller, M. C. & Miller, G. Resolving the paradox of common, harmful, heritable mental disorders: which evolutionary genetic models work best? *Behav. Brain Sci.* **29**, 385–404 (2006).
48. Mullins, N. et al. Reproductive fitness and genetic risk of psychiatric disorders in the general population. *Nat. Commun.* **8**, 15833 (2017).
49. Ware, J. J. et al. Genome-wide meta-analysis of cotinine levels in cigarette smokers identifies locus at 4q13.2. *Sci. Rep.* **6**, 20092 (2016).
50. Burgess, S. et al. Network Mendelian randomization: using genetic variants as instrumental variables to investigate mediation in causal pathways. *Int. J. Epidemiol.* **44**, 484–495 (2014).
51. Schoeck, A. et al. Quantification of frequency-dependent genetic architectures and action of negative selection in 25 UK Biobank traits. Preprint at bioRxiv <https://doi.org/10.1101/188086> (2017).
52. Mokry, L. E. et al. Vitamin D and risk of multiple sclerosis: a Mendelian randomization study. *PLoS Med.* **12**, e1001866 (2015).
53. Gamazon, E. R. et al. A gene-based association method for mapping traits using reference transcriptome data. *Nat. Genet.* **47**, 1091–1098 (2015).
54. Gusev, A. et al. Integrative approaches for large-scale transcriptome-wide association studies. *Nat. Genet.* **48**, 245–252 (2016).
55. Zhu, Z. et al. Integration of summary data from GWAS and eQTL studies predicts complex trait gene targets. *Nat. Genet.* **48**, 481–487 (2016).
56. GTEx Consortium et al. Genetic effects on gene expression across human tissues. *Nature* **550**, 204–213 (2017).
57. Lyall, D. M. et al. Association of body mass index with cardiometabolic disease in the UK Biobank: a Mendelian randomization study. *JAMA Cardiol.* **2**, 882–889 (2017).

Acknowledgements

We are grateful to B. Neale, S. Raychaudhuri, C. Patel, S. Kathiresan, B. Pasaniuc, and H. Finucane for helpful discussions and to P.-R. Loh and S. Gazal for producing BOLT-LMM summary statistics for UK Biobank traits. This research was conducted using the UK Biobank Resource under Application #16549 and was funded by National Institutes of Health grants R01 MH107649, U01 CA194393, and R01 MH101244.

Author contributions

L.J.O. and A.L.P. conceived the methods, designed the analyses, and wrote the manuscript. L.J.O. performed the analyses.

Competing interests

The authors declare no competing interests.

Additional information

Supplementary information is available for this paper at <https://doi.org/10.1038/s41588-018-0255-0>.

Reprints and permissions information is available at www.nature.com/reprints.

Correspondence and requests for materials should be addressed to L.J.O. or A.L.P.

Publisher's note: Springer Nature remains neutral with regard to jurisdictional claims in published maps and institutional affiliations.

© The Author(s), under exclusive licence to Springer Nature America, Inc. 2018

Methods

LCV model. The LCV random effects model assumes that the distribution of marginal effect sizes for the two traits can be written as the sum of two independent bivariate distributions (visualized in Fig. 1c–e in orange and blue, respectively): (1) a shared genetic component ($q_1\pi, q_2\pi$) whose values are proportional for both traits, and (2) an even genetic component (γ_1, γ_2) whose density is mirror symmetric across both axes. Distribution 1 resembles a line through the origin, and we interpret its effects as being mediated by an LCV (L) (Fig. 1a); distribution 2 does not contribute to the genetic correlation, and we interpret its effects as direct effects. Informally, the LCV model assumes that any asymmetry in the shared genetic architecture arises from the action of a latent variable.

In detail, the LCV model assumes that there exist scalars q_1, q_2 and a distribution $(\pi, \gamma_1, \gamma_2)$ such that

$$(\alpha_1, \alpha_2) = (q_1\pi + q_2\pi) + (\gamma_1, \gamma_2) \quad (3)$$

where $\pi \perp (\gamma_1, \gamma_2)$ and $(\gamma_1, \gamma_2) \sim (-\gamma_1, \gamma_2) \sim (\gamma_1, -\gamma_2)$. Here α_k is the random marginal effect of a SNP of trait k , π is interpreted as the marginal effect of a SNP on L , and γ_k is interpreted as the non-mediated effect of a SNP on trait k . α and π (but not γ) are normalized to have unit variance, and all random variables have zero mean. (The symbol \sim means ‘has the same distribution as.’) q_1, q_2 are the model parameters of primary interest, and we can relate them to the mixed fourth moments, which are observable (equation (2)). In particular, this implies that the model is identifiable (except when the excess kurtosis $\kappa_\pi = 0$; see Supplementary Note). We do not expect that κ_π will be exactly zero for any real trait, but there will be lower power for traits with higher polygenicity. Note that we have avoided assuming any particular parametric distribution.

The LCV model assumptions are strictly weaker than the assumptions made by MR. Like LCV, a formulation of the MR assumptions is that the bivariate distribution of SNP effect sizes can be expressed in terms of two distributions. In particular, it assumes that the effect-size distribution is a mixture of (1') a distribution whose values are proportional for both traits (representing all SNPs that affect the exposure Y_1) and (2') a distribution with zero values for the exposure Y_1 (representing SNPs that only affect the outcome Y_2). These two distributions can be compared with distributions 1 and 2 above. Because 1' is identical to 1 and 2' is a special case of 2', the LCV model assumptions are strictly weaker than the MR assumptions (indeed, much weaker). We also note that the MR model is commonly illustrated with a non-genetic confounder affecting both traits. Our latent variable L is a genetic variable, and it is not analogous to the non-genetic confounder. Similar to MR, LCV is unaffected by non-genetic confounders (such a confounder may result in a phenotypic correlation that is unequal to the genetic correlation).

The GCP is defined as:

$$\text{GCP} = \frac{\log |q_2| - \log |q_1|}{\log |q_2| + \log |q_1|} \quad (4)$$

which satisfies equation (1). GCP is positive when trait 1 is partially genetically causal for trait 2. When $\text{GCP} = 1$, trait 1 is fully genetically causal for trait 2: $q_1 = 1$ and the causal effect size is $q_2 = \rho_g$ (Fig. 1b,e). The LCV model is broadly related to dimension reduction techniques such as factor analysis³⁸ and independent components analysis³⁹, although it differs in its modeling assumptions as well as its goal (causal inference); our inference strategy (mixed fourth moments) also differs.

Under the LCV model assumptions, we derive the estimation equation (2) as follows:

$$\begin{aligned} E(\alpha_1^3\alpha_2) &= E((\gamma_1 + q_1\pi)^3(\gamma_2 + q_2\pi)) \\ &= q_1^3q_2E(\pi^4) + 3q_1q_2E(\pi^2\gamma_1^2) \\ &= q_1^3q_2E(\pi^4) + 3q_1q_2E(\pi^2)E(\gamma_1^2) \\ &= q_1^3q_2E(\pi^4) + 3q_1q_2(1 - q_1^2) \\ &= q_1^3q_2(E(\pi^4) - 3) + 3q_1q_2 \end{aligned}$$

In the second line, we used the independence assumption to discard cross-terms of the form $\gamma_1\pi^3$ and $\gamma_1^3\pi$, and we used the symmetry assumption to discard terms of the form $\gamma_1\gamma_2^3$. In the third and fourth lines, we used the independence assumption, which implies that $E(\gamma_1^2\pi^2) = E(\gamma_1^2)E(\pi^2) = E(\gamma_1^2) = 1 - q_1^2$. The factor $E(\pi^4) - 3$ is the excess kurtosis of π , which is zero when π follows a Gaussian distribution; for the estimation equation to be useful, $E(\pi^4) - 3$ must be non-zero (see Supplementary Note).

Estimation under the LCV model. To estimate the GCP and to test for partial causality, we use six steps. First, we use LD score regression¹⁹ to estimate the heritability of each trait; these estimates are used to normalize the summary statistics. Second, we apply cross-trait LD score regression¹⁶ to estimate the genetic correlation; the intercept in this regression is also used to correct for possible sample overlap when estimating the mixed fourth moments. Third, we estimate the

mixed fourth moments of the bivariate effect-size distribution. Fourth, we compute test statistics for each possible value of the GCP, based on the estimated genetic correlation and on the estimated mixed fourth moments. Fifth, we jackknife on these test statistics to estimate their standard errors, similar to ref.¹⁹, obtaining a likelihood function for the GCP. Sixth, we obtain posterior means and standard errors for the GCP using this likelihood function and a uniform prior distribution. These steps are detailed below.

First, we apply LD score regression to normalize the test statistics. Under the LCV model, the marginal effect sizes for each trait, α_1 and α_2 , have unit variance. We use a slightly modified version of LD score regression¹⁹ with LD scores computed from UK10K data⁴⁰. In particular, we run LD score regression using a slightly different weighting scheme, matching the weighting scheme in our mixed fourth moment estimators; the weight of SNP i was:

$$w_i = \max \left(1, \frac{1}{\ell_i^{\text{HapMap}}} \right) \quad (5)$$

where ℓ_i^{HapMap} was the estimated LD score between SNP i and other HapMap3 SNPs (this is approximately the set of SNPs that were used in the regression). This weighting scheme is motivated by the fact that SNPs with high LD to other regression SNPs will be over-counted in the regression (see ref.¹⁹).

Similar to ref.¹⁶, we improve power by excluding large-effect variants when computing the LD score intercept; for this study, we chose to exclude variants with χ^2 statistic $30\times$ the mean, exploiting the fact that genome-wide significant SNPs are not due to population stratification (these variants are not excluded in subsequent steps). Then, we divide the summary statistics by $s = \sqrt{\chi_{\text{avg}}^2 - \chi_0^2}$, where χ_{avg}^2 is the weighted mean χ^2 statistic and χ_0^2 is the LD score intercept, obtaining estimates $\hat{\alpha}$ of α . (We also divide the LD score intercept by s^2 .) We assess the significance of the heritability by performing a block jackknife on s , defining the significance Z_h as s divided by its estimated standard error.

Second, to estimate the genetic correlation, we apply cross-trait LD score regression¹⁶. Similar to the procedure described above, we use a slightly modified weighting scheme (equation (5)), and we exclude large-effect variants when computing the cross-trait LD score intercept. We assess the significance of the genetic correlation using a block jackknife.

Third, we estimate the mixed fourth moments $E(\alpha_1\alpha_2^3)$ using the following equation:

$$E(\hat{\alpha}_1\hat{\alpha}_2^3|\alpha_1, \alpha_2) = \alpha_1\alpha_2^3 + 3\alpha_1\alpha_2\sigma_2^2 + \alpha_2^2\sigma_{12} + 3\sigma_{12}\sigma_2^2 \quad (6)$$

where σ_2^2 is the LD score regression intercept for trait 2 (normalized by dividing by s_2^2) and σ_{12} is the cross-trait LD score regression intercept (normalized by dividing by s_1s_2). For simulations with no LD, we fix $\sigma_2^2 = 1/s_2^2$ and $\sigma_{12} = 0$. Thus, we obtain an estimate $\hat{\kappa}_k$ of $\kappa_k = E(\alpha_k^2\alpha_1\alpha_2) - 3\rho_g$ by computing the weighted average of $\hat{\alpha}_1\hat{\alpha}_2^3$ over SNPs (with weights given by equation (5)) and subtracting $3\hat{\alpha}_1\hat{\alpha}_2\sigma_2^2 + \hat{\alpha}_2^2\sigma_{12} + 3\sigma_{12}\sigma_2^2$.

Fourth, we define a collection of statistics $S(x)$ for $x \in X = \{-1, -0.01, -0.02, \dots, 1\}$ (corresponding to possible values of GCP):

$$S(x) = \frac{A_1(x) - A_2(x)}{\max \left(\frac{1}{|\rho_g|}, \sqrt{A_1(x)^2 + A_2(x)^2} \right)} \quad (7)$$

where $A_k(x) = |\rho_g|^{-x} \hat{\kappa}_k$. The motivation for utilizing the normalization by $\sqrt{A_1(x)^2 + A_2(x)^2}$ is that the magnitudes of $A_1(x)$ and $A_2(x)$ tend to be highly correlated, leading to greatly increased standard errors if we only use the numerator of S . However, the denominator tends to zero when the genetic correlation is zero, leading to instability in the test statistic and false positives. The use of the threshold leads to conservative, rather than inflated, standard errors when the genetic correlation is zero or nearly zero. We recommend only analyzing trait pairs with a significant genetic correlation, and this threshold usually has no effect on the results. Another reason not to analyze trait pairs whose genetic correlation is non-significant is that, for positive LCV results, the genetic correlation provides critical information about the causal effect size and direction.

Fifth, we estimate the variance of $S(x)$ using a block jackknife with $k = 100$ blocks of contiguous SNPs, resulting in minimal non-independence between blocks. Blocks are chosen to include the same number of SNPs, and the jackknife variance is:

$$\sigma_{S(x)}^2 = 101 \sum_{j=1}^{100} (S_j(x) - S_{\text{avg}}(x))^2 \quad (8)$$

where $S_j(x)$ is the test statistic computed on blocks $1, \dots, j-1, j+1, \dots, 100$ and $S_{\text{avg}}(x)$ is the mean of the jackknife estimates. We compute an approximate likelihood, $L(S|GCP=x)$, by assuming (1) that $L(S|GCP=x) = L(S(x)|GCP=x)$ and (2) that if $GCP=x$, then $S(x)/\sigma_{S(x)}$ follows a T distribution with 98 degrees of freedom.

Sixth, we impose a uniform prior on the GCP, enabling us to obtain a posterior mean estimate:

$$\widehat{\text{GCP}} = \frac{1}{|X|} \sum_{x \in X} xL(x) \quad (9)$$

The estimated standard error is

$$\widehat{\text{SE}} = \frac{1}{|X|} \sum_{x \in X} (S_j(x) - S_{\text{avg}}(x))^2 L(x) \quad (10)$$

To compute P values, we apply a t -test to the statistic $S(0)$.

Outlier removal. In a secondary analysis, we applied an outlier removal procedure to determine whether our results on real traits using LCV were unduly influenced by individual loci. We computed the LCV test statistic $S(0)$ for each of the 100 jackknife blocks, discarded jackknife blocks that were >20 standard deviations from the mean, and reran the procedure iteratively until no outliers remained. For most trait pairs, this process results in the removal of no blocks; for a handful of trait pairs, it results in the removal of one or a few.

We do not recommend the broad use of this procedure, because outlier loci may contain valuable information. In particular, if any SNP affects trait 1 without affecting trait 2 proportionally, this suggests that trait 1 is not causal for trait 2.

An alternative explanation is that its effect on trait 2 is masked by an opposing pleiotropic effect, either of the same causal SNP or of a different causal SNP at the same locus. If an outlier locus is to be removed, we recommend manually examining it and determining whether its removal can be justified or whether it provides competing statistical evidence against a causal effect.

Reporting Summary. Further information on research design is available in the Nature Research Reporting Summary linked to this article.

Code availability. Open-source software implementing our method is available at <https://github.com/lukejoconnor/LCV>.

Data availability

UK Biobank summary statistics are publicly available at <http://data.broadinstitute.org/alkesgroup/UKBB/>.

References

- 58. Child, D. *The Essentials of Factor Analysis*. (A&C Black, London, 1990).
- 59. Comon, P. Independent component analysis, a new concept? *Signal Process.* **36**, 287–314 (1994).
- 60. UK10K Consortium. The UK10K project identifies rare variants in health and disease. *Nature* **526**, 82–90 (2015).

Reporting Summary

Nature Research wishes to improve the reproducibility of the work that we publish. This form provides structure for consistency and transparency in reporting. For further information on Nature Research policies, see [Authors & Referees](#) and the [Editorial Policy Checklist](#).

Statistical parameters

When statistical analyses are reported, confirm that the following items are present in the relevant location (e.g. figure legend, table legend, main text, or Methods section).

- | | |
|-------------------------------------|--|
| n/a | Confirmed |
| <input checked="" type="checkbox"/> | The exact sample size (<i>n</i>) for each experimental group/condition, given as a discrete number and unit of measurement |
| <input checked="" type="checkbox"/> | An indication of whether measurements were taken from distinct samples or whether the same sample was measured repeatedly |
| <input type="checkbox"/> | The statistical test(s) used AND whether they are one- or two-sided
<i>Only common tests should be described solely by name; describe more complex techniques in the Methods section.</i> |
| <input type="checkbox"/> | A description of all covariates tested |
| <input type="checkbox"/> | A description of any assumptions or corrections, such as tests of normality and adjustment for multiple comparisons |
| <input type="checkbox"/> | A full description of the statistics including central tendency (e.g. means) or other basic estimates (e.g. regression coefficient) AND variation (e.g. standard deviation) or associated estimates of uncertainty (e.g. confidence intervals) |
| <input type="checkbox"/> | For null hypothesis testing, the test statistic (e.g. <i>F</i> , <i>t</i> , <i>r</i>) with confidence intervals, effect sizes, degrees of freedom and <i>P</i> value noted
<i>Give P values as exact values whenever suitable.</i> |
| <input type="checkbox"/> | For Bayesian analysis, information on the choice of priors and Markov chain Monte Carlo settings |
| <input type="checkbox"/> | For hierarchical and complex designs, identification of the appropriate level for tests and full reporting of outcomes |
| <input type="checkbox"/> | Estimates of effect sizes (e.g. Cohen's <i>d</i> , Pearson's <i>r</i>), indicating how they were calculated |
| <input type="checkbox"/> | Clearly defined error bars
<i>State explicitly what error bars represent (e.g. SD, SE, CI)</i> |

Our web collection on [statistics for biologists](#) may be useful.

Software and code

Policy information about [availability of computer code](#)

Data collection

No code was used for data collection.

Data analysis

Data analysis was performed using LCV software (<https://github.com/lukejocnnon/LCV>).

For manuscripts utilizing custom algorithms or software that are central to the research but not yet described in published literature, software must be made available to editors/reviewers upon request. We strongly encourage code deposition in a community repository (e.g. GitHub). See the Nature Research [guidelines for submitting code & software](#) for further information.

Data

Policy information about [availability of data](#)

All manuscripts must include a [data availability statement](#). This statement should provide the following information, where applicable:

- Accession codes, unique identifiers, or web links for publicly available datasets
- A list of figures that have associated raw data
- A description of any restrictions on data availability

All GWAS summary statistics used in this paper is publicly available. In particular, UK Biobank summary statistics were described in Loh et al. 2018 NG and are publicly available (see Data Availability).

Field-specific reporting

Please select the best fit for your research. If you are not sure, read the appropriate sections before making your selection.

Life sciences

Behavioural & social sciences

Ecological, evolutionary & environmental sciences

For a reference copy of the document with all sections, see nature.com/authors/policies/ReportingSummary-flat.pdf

Life sciences study design

All studies must disclose on these points even when the disclosure is negative.

Sample size GWAS datasets were selected based on the statistical significance of their LDSC heritability estimate, as described.

Data exclusions GWAS datasets were excluded based on the statistical significance of their LDSC heritability estimate and based on pairwise genetic correlations, as described.

Replication The results are fully reproducible.

Randomization We did not perform any experiments that involved assigning individuals to groups.

Blinding We did not perform any experiments that involved assigning individuals to groups.

Reporting for specific materials, systems and methods

Materials & experimental systems

n/a	Involved in the study <input checked="" type="checkbox"/> Unique biological materials <input checked="" type="checkbox"/> Antibodies <input checked="" type="checkbox"/> Eukaryotic cell lines <input checked="" type="checkbox"/> Palaeontology <input checked="" type="checkbox"/> Animals and other organisms <input checked="" type="checkbox"/> Human research participants
-----	--

Methods

n/a	Involved in the study <input checked="" type="checkbox"/> ChIP-seq <input checked="" type="checkbox"/> Flow cytometry <input checked="" type="checkbox"/> MRI-based neuroimaging
-----	---